

INFLUENCE OF MgO ON MICROSTRUCTURAL AND MECHANICAL PROPERTIES OF RAW CLAY FROM BURKINA FASO

**Mohamed Seynou^{1*}, Younoussa Millogo², Lamine Zerbo¹,
Raguilnaba Ouedraogo¹**

¹*Université de Ouagadougou, UFR/ Sciences Exactes et Appliquées,
Departement de Chimie, 03 B.P. 7021 Ouagadougou 03, Burkina Faso*

²*Université Polytechnique de Bobo-Dioulasso, Institut des Sciences de la
Nature et de la Vie (ISNV), 01 BP 1091 Bobo 01, Burkina Faso*

*Corresponding author: seynou1mohamed@yahoo.fr

Received: February, 07, 2014

Accepted: May, 05, 2014

Abstract: The influence of MgO on mechanical and microstructural properties of raw clay material from Burkina Faso was investigated by means of X-ray diffraction, scanning electron microscopy, infrared spectroscopy, differential thermal analysis and numerical simulation. The mineralogical composition was modified with the formation of new crystalline phases such as mullite, spinel – Mg, enstatite and forsterite. During the sintering and with add of MgO, the mullite quantity decrease contrary to forsterite and affect the different properties of sintered products. The mechanical properties were improved with MgO amount around 2 – 5 wt%. For magnesia amount higher than 5 wt%, the magnesia is not entirely consumed and is originated to the formation of pores in the manufactured products which are detrimental to the mechanical properties.

Keywords: *forsterite, mechanical properties, mullite, surface responses*

INTRODUCTION

Cordierite ($2\text{MgO}\cdot 2\text{Al}_2\text{O}_3\cdot 5\text{SiO}_2$) [1-5] and forsterite (Mg_2SiO_4) [5-7] are recently greatly used in ceramic and electronic fields. They present innovative and interesting properties [8]. Cordierite is thermodynamically stable as indicated its mechanical strength 250 MPa on the previous study [4]. It improves the mechanical properties of sintered products. Its low dielectric constant (5.0 to 1 MHz) permits it to be used in the packaging of electronic materials [4]. Forsterite is very used in the electric furnaces due to its refractory character (melting point 1890 °C) [6]. It has a low electrical conductivity which allows its use in the manufacture of laser tunnels [7].

These minerals phase (cordierite and forsterite) are produced by sol-gel technique or directly during a sintering of a raw material containing the oxides SiO_2 , Al_2O_3 and MgO . The sol-gel technique is difficult and expensive. We have then chosen the sintering method of the raw clay materials.

The main purpose of this study is to follow the evolution of mineralogical, microstructural and mechanical properties of raw clay from Burkina Faso in the contribution of magnesia. A numerical simulation of the mechanical behavior was made to optimize the use of the magnesia.

MATERIALS AND METHODS

Materials

The basic used materials were clay deposit in Korona (Burkina Faso) and magnesia as additive. The Korona clay has been characterized in our previous work [9]. It is composed mainly by kaolinite, quartz, albite and orthoclase. At major phases are added talc, hematite and goethite in low quantity. Magnesia provided by Merck (98% purity) contains (Figure 1) mainly magnesia (MgO) and a small amount of magnesite (MgCO_3). The chemical composition of the two materials is summarized in Table 1. The high content of Al_2O_3 and SiO_2 indicates the presence of aluminosilicate and is interesting for cordierite and forsterite synthesis. The relatively important amount of Na_2O and K_2O are due to the presence of feldspar component (albite and orthoclase) and the significant amount of iron oxide is ascribable to the goethite and hematite in the sample. The loss on ignition of magnesia powder is used to evaluate the rate of magnesite MgCO_3 (6%) and magnesia MgO (94%).

Table 1. Chemical analysis (wt%) of the starting materials:
Korona and Magnesia powder

Oxides	Al_2O_3	SiO_2	Fe_2O_3	Na_2O	K_2O	CaO	MgO	TiO_2	L.O.I
Korona	20.3	57.2	6.53	1.49	2.91	0.99	1.12	0.71	7.52
Magnesia	-	-	-	-	-	-	97	-	3

- : not detected, L.O.I : Loss on ignition at 1000 °C

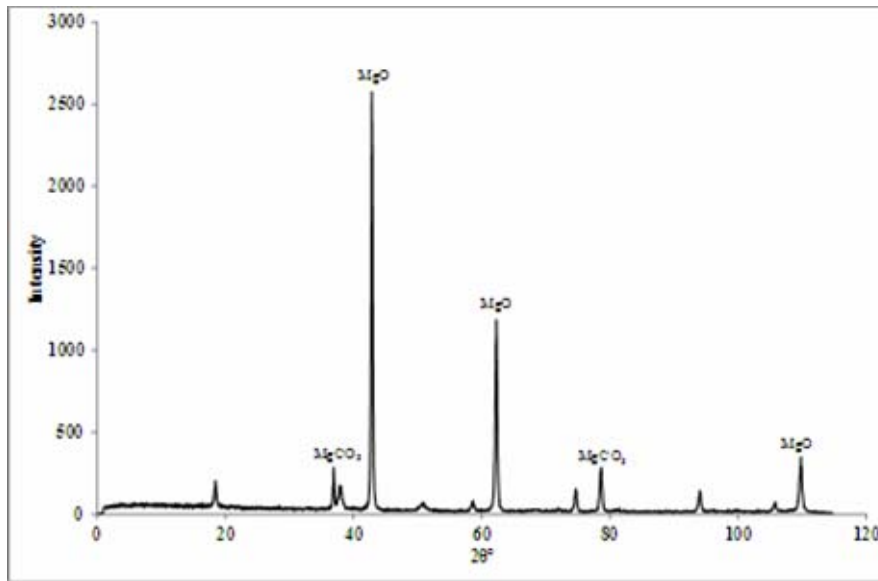


Figure 1. X-ray diffraction pattern of magnesia powder

Preparation of specimens

The mixtures constituted by raw material, magnesia and water (water / material = 0.5) were grounded until the grain size < 63 μm . For the elaboration of specimen (10 cm x 4 cm x 1 cm), crushed mixtures were humidified (average 5 mass %) and pressed at 15 MPa. After being soaked, the obtained bars were dried for 24 h at 110 $^{\circ}\text{C}$, and fired during 60 min. The heating rate and the sintering temperature were 10 $^{\circ}\text{C}/\text{min}$ and 1100 $^{\circ}\text{C}$ respectively.

Characterization of sintered specimen

The flexural strength σ (3 points technique) was evaluated using the following equation:

$$\sigma = \frac{3FE}{2le^2} \quad (1)$$

where: F - applied force, E - distance between the two supports, l - the width of the bar, e - the thickness.

The water absorption values were determined by the mass difference observed between the as-fired and water saturated samples.

The X-ray diffractions (XRD) of fired samples at 1100 $^{\circ}\text{C}$ were performed with a diffractometer Brüker D 5000 with back graphite using $\text{CuK}\alpha$ radiation and operating at 40 kV and 50 mA. The diffractograms were treated with Diffracplus D Quant software.

The infrared spectra were recorded in the range of 400 - 4000 cm^{-1} using a Perkin Elmer FT-IR Spectrometer. Each sample (5 mg) was mixed with 500 mg of KBr and pressed into disc under vacuum using 5 tons and 10 tons as pressure and during 5 minutes.

The differential thermal analysis (DTA/TG) was carried out using SETARAM instrument operating at 10 $^{\circ}\text{C}/\text{min}$ from ambient to 1200 $^{\circ}\text{C}$. Calcined alumina was taken as a reference.

The image examinations of fractured surfaces of sintered samples were performed with the Hitachi S2500 scanning electron microscopy.

Simulation

The effect of two factors, namely magnesia percentage in the specimen (X_1) and sintering temperature of the specimens (X_2), on the compressive strength (Y_1) and water absorption (Y_2) of the sintered products has been studied in order to determine the best experimental conditions. This has been accomplished by applying surface responses methodology (RSM) and desirability approach. In order to achieve this purpose, the composite design with star for two factors was adopted as experience matrix. The design (Figure 2) is composed by four (4) experimental points corresponding to the four corners of a square, one (1) experimental point corresponding to the center of the square and four (4) experimental points on the axes at a distance α from the center. Center experience was repeated three times to check the experiments reproducibility [10]. To meet the criterion of almost orthogonality we took $\alpha = 1.21$.

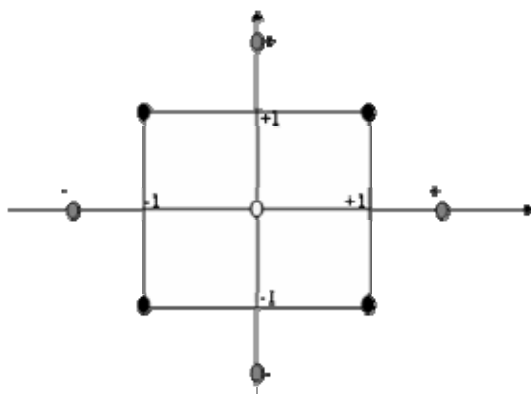


Figure 2. Distribution of the experimental points in the two variables composite design

The experiment matrix is composed then by 12 experiments (Table 2).

Table 2. Matrix design for two variables

N° EXP	1	2	3	4	5	6	7	8	9	10	11	12
X_1	-1.00	1.00	-1.00	1.00	0	0	-1.21	1.21	0	0	0	0
X_2	-1.00	-1.00	1.00	1.00	0	0	0	0	-1.21	1.21	0	0

For predicting the optimal conditions, a second order polynomial function is fitted to correlate relationship between independent variables and response. For two factors this equation is:

$$Y_{calc} = b_0 + b_1 X_1 + b_2 X_2 + b_{12} X_1 X_2 + b_{11} X_1^2 + b_{22} X_2^2 \quad (2)$$

where:

- X_1 and X_2 are the values of coded variables;
- b_0 is the theoretical value of the response at the center of the field experiment;
- b_1 and b_2 are a model coefficients respectively measuring the effect of MgO content and temperature on the response;

- b_{11} and b_{22} are a model coefficients describing the shape of the curve (stationary points);
- b_{12} is a coefficient measuring the effect of interaction between the two factors;
- Y_{calc} is the calculated response;
- Y_{exp} is the response measured, $Y_{exp} = Y_{calc} + e$, with e the Error.

NEMROD software (New Efficient Methodology for Research using Optimal Design) was used to calculate the various coefficients.

RESULTS AND DISCUSSION

Mineralogy

X- ray diffraction patterns of the sintered specimen at 1100 °C are plotted in Figure 3. Without magnesia, the specimen is characterized by the formation of mullite in important amount. Magnesium phases (forsterite and enstatite) are also presented in the same specimen in lesser quantities. These phases provide on the decomposition of talc present in the raw material. With magnesia, Mg-spinel, forsterite and enstatite phases are formed. Their quantities increased with magnesia amount, contrary to mullite quantities. The periclase was also observed in all products with magnesia. It provides on enstatite transformation into forsterite. According to Brindley and Hayami [11], during the reaction between MgO and SiO₂, enstatite is first formed and followed by forsterite by interlayer diffusion of MgO.

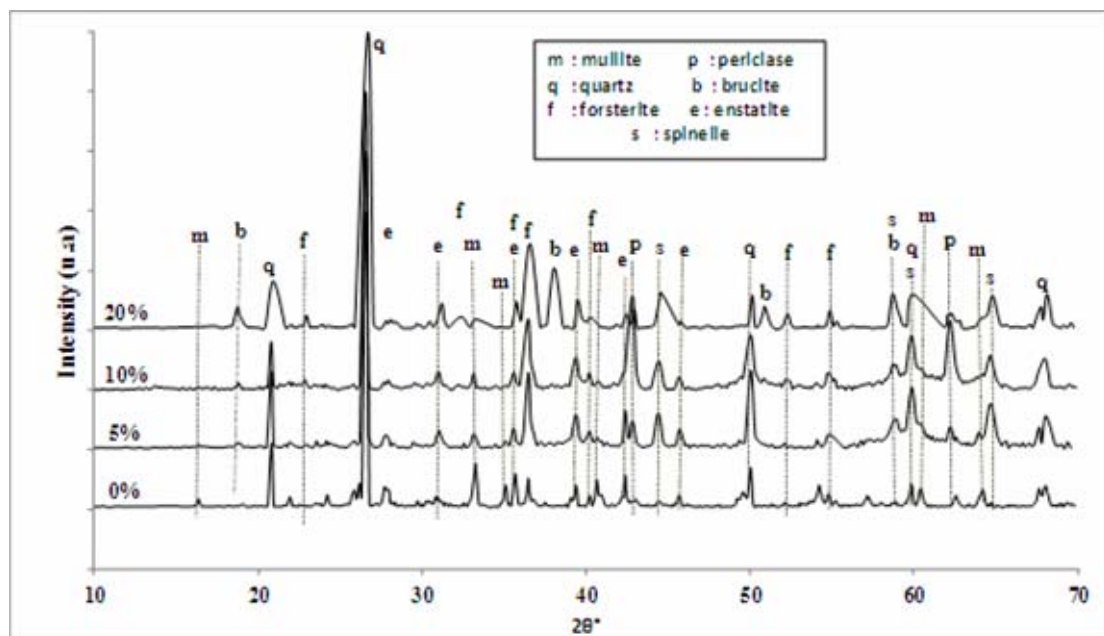


Figure 3. X-ray diffraction pattern of sintered specimen at 1100 °C

Infrared spectrometry results (Figure 4) are corroborated with the X-ray results. The double band of quartz (798 and 778 cm⁻¹) is transformed with addition of magnesia into

a single band and decrease progressively in intensity. This transformation shows the reaction between the magnesia and quartz. The loss of quartz band at 550 cm^{-1} confirmed the reaction of quartz with magnesia. The new bands located at 615 and 840 cm^{-1} characteristic of Mg-O bond [12] are due to the formation of new magnesium phases namely forsterite and Mg-spinel. Enstatite formation is indicated by the splitting of band at 693 cm^{-1} . The bands at 512 and 963 cm^{-1} (Mg-O) are present only with 10 and 20 wt% of MgO, they characterize the part of magnesia remained in the sintered specimen. With 5 wt%, all magnesia is consumed. The presence of remaining magnesia for 10 and 20 wt% of added magnesia is confirmed by the appearance of the band at 1440 cm^{-1} attributable to CO_3^{2-} [13] of magnesite. The band at 1082 cm^{-1} is characteristic of mullite formation.

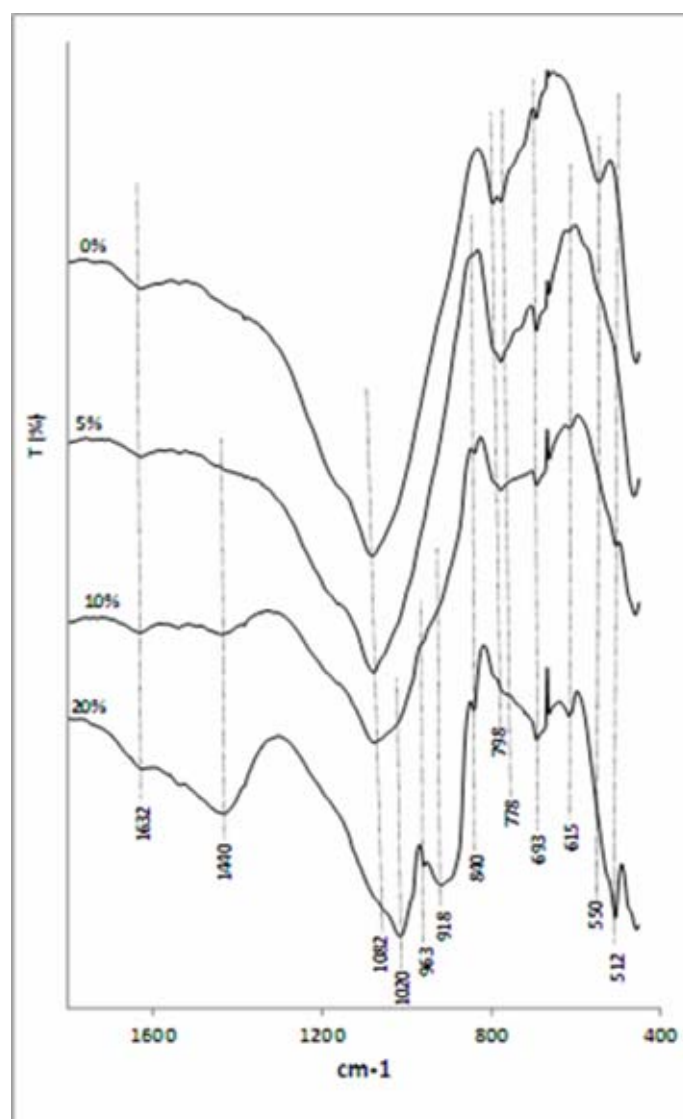


Figure 4. IR spectra of sintered specimens at $1100\text{ }^{\circ}\text{C}$

Figure 5 presents the thermal analysis (DTA / TG) results of sintered specimens. These results confirm the XRD and IR results. The first endothermic peak around $120\text{ }^{\circ}\text{C}$ was

assigned to the loss of hydration water. The second endothermic peak at 420 °C corresponds to dehydroxylation of brucite and recrystallization of magnesia. This loss corresponds to 3.25 wt% for the specimen with 20 wt% magnesia and 0.25 wt% for the specimen with 5 wt% of magnesia. The third endothermic peak at 573 °C corresponds to the allotropic transformation of quartz α to quartz β . Four exothermic peaks respectively at 720, 769, 830 and 885 °C are present in the specimen with 20 wt% of magnesia and are characteristic of magnesium phases. These phases are respectively magnesite, Mg-spinel phase, enstatite and forsterite [14, 15].

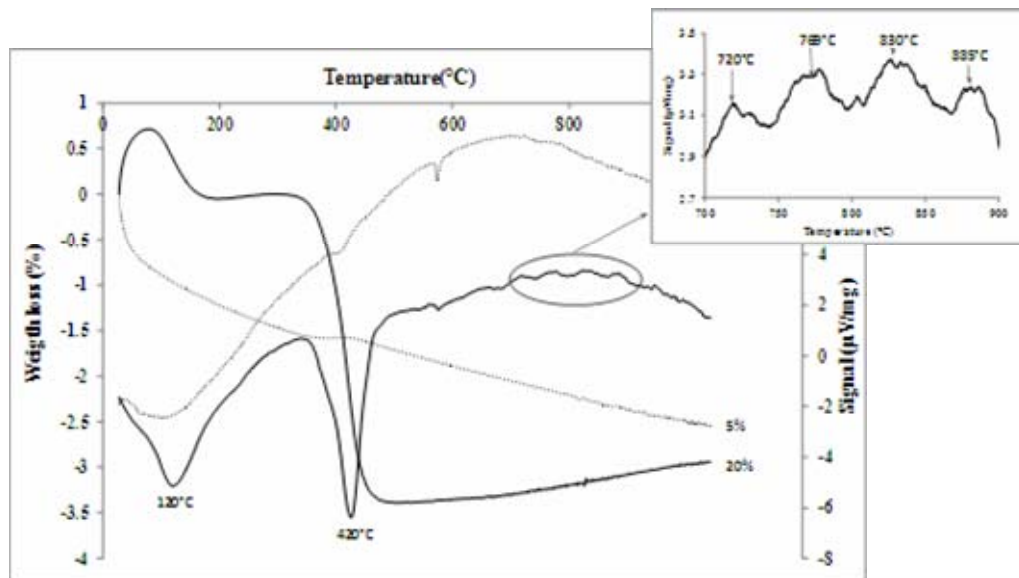


Figure 5. DTA / TG analysis of sintered specimen at 1100 °C

Microstructure

SEM images of the fractured surface of different specimen at 1100 °C are presented in Figure 6. With the magnification X1000 (Figure 6a), we can discuss on the porosity of the sintered specimens. The shade without addition of magnesia indicates the presence of liquid phase with no connected small pores. With 5 wt% of magnesia, the microstructure is modified by forming a highly consolidated material which is characterized by absence of pores. With 10 and 20 wt% of magnesia as additive, we have the formation of inter-connected larger pores. We also note the presence of very small white grain size. With high magnification X10000 (Figure 6b), we can discuss on the structure of the formed phases. The SEM image of the specimen without magnesia shows a pile of fiber in large quantities corresponding to mullite. With 5 wt%, the SEM image is characterized by a small amount of fiber (mullite) bathed in a matrix composed of small granular phase (spinel). The SEM image with 10 wt% addition is characterized by a stack of small platelets (0.5 μm in diameter) corresponding to the forsterite. With the 20 wt% we note an image similar to the 10 wt% but less stacked platelets.

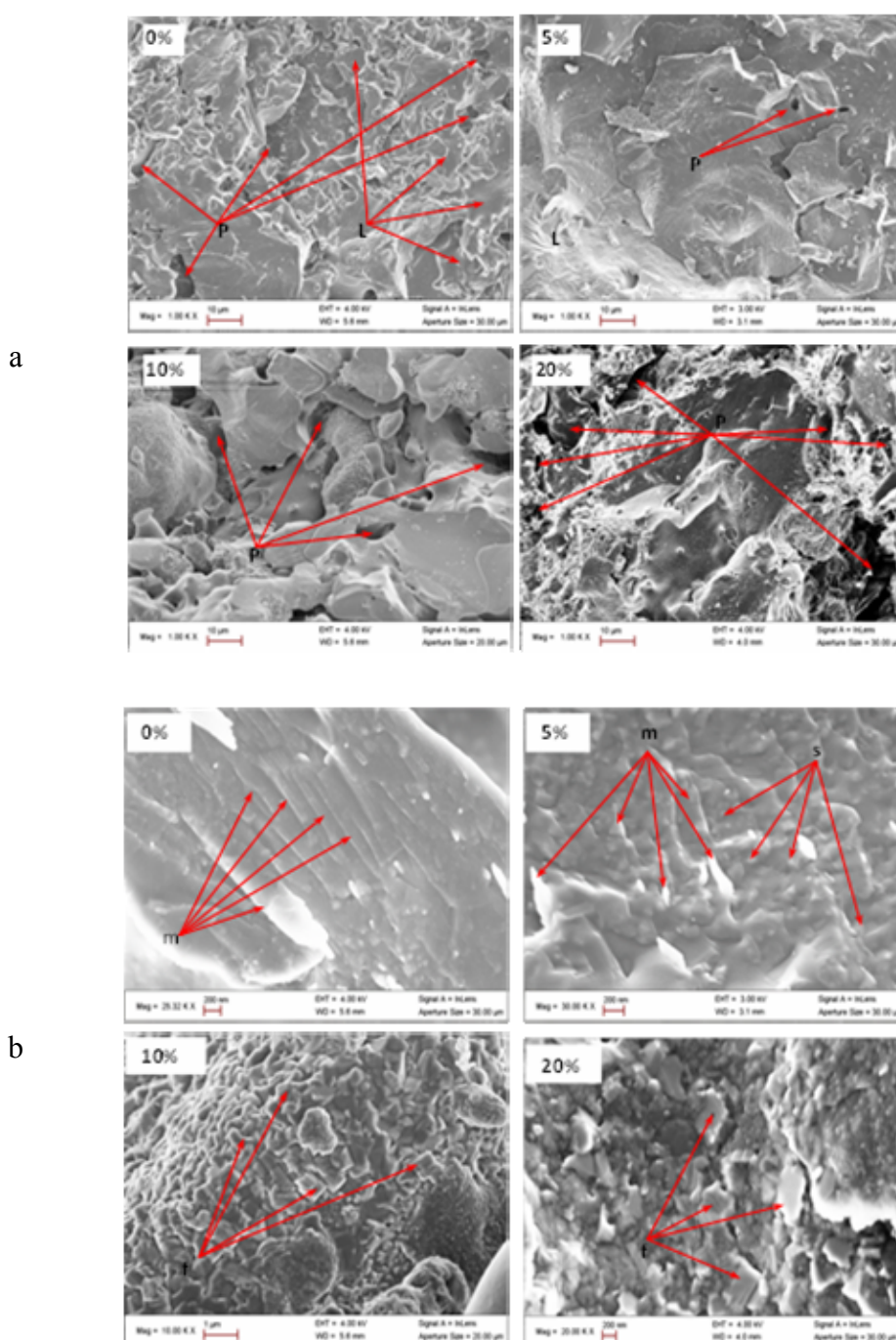


Figure 6. SEM images of fractured surface of sintered specimen at 1100 °C
m: mullite, s: Mg-spinelle, f: forsterite, L: liquid phase, P: pore
 (a - with the magnification X1000, b - with high magnification X10000)

Physical and mechanical properties

The flexural strength of specimens is reported in Table 3. The strength increase with magnesia amount until 5 wt%. Above this percentage, the strength decreased gradually. These results were predictable in terms of mineralogical composition and microstructure

properties. The high amount of formed forsterite at the expense of mullite is responsible for the reduction of mechanical strength. Water absorption evolution is in accordance with the mechanical strength. It is lower with magnesia, which corresponds also to the greater mechanical strength. Above 5 wt% MgO, the water absorption increases rapidly.

Table 3. Mechanical properties of specimen sintered at 1100 °C

MgO (wt%)	0	5	10	20
Flexural strength (MPa)	35	39.5	23	12.5
Water absorption (%)	5.5	4	8.75	15

This growth is explained by the presence in these materials of magnesia which didn't react and by the presence of large pores which have been shown by SEM images.

Optimization of the mechanical properties

The influence of temperature and the magnesia amount on the mechanical properties has been studied by numerical simulation. The explored experimental domain and the levels attributed to each variable are given in Table 4. Two responses, strength (Y_1) and water absorption (Y_2) of sintered products, were explored. The model coefficients determined with the NEMROD Software permit to have the equation of each response.

Table 4. Variables and experimental domain

Levels	-1.21	-1	0	+1	+1.21
Percentage of MgO X_1 (%)	-1.05	0	5	10	11.05
Sintering temperature X_2 (°C)	1039.5	1050	1100	1150	1160.5

Mechanical strength

The obtained relationship between the strength and the previously mentioned two factors is give by the equation 3.

$$Y_1 = 39.80 - 7.46X_1 + 12.15X_2 - 5.98X_1 * X_2 + 2.06X_1^2 - 2.88X_2^2 \quad (3)$$

The negative sign of the coefficient (-7.46) relevant to the magnesia percentage indicates that the magnesium content has an antagonistic effect on the mechanical strength. Strength decreases with increasing of magnesia content. Coefficient relevant to temperature is positive (12.15) and indicates a synergistic effect of temperature on strength. The strength increases with temperature increasing. The quadratic coefficient (2.06 and -2.88) indicates the presence of stationary points. The iso-response curve (Figure 7) shows the evolution of strength as a function of temperature and magnesia percentage. It confirms the presence of stationary point around 2 to 3 wt% of MgO.

Water absorption

The relationship between the water absorption and the two factors is give by the equation 4.

$$Y_2 = 3,96 + 1,89X_1 - 3,18X_2 + 2,10X_1 * X_2 + 0,55X_1^2 + 0,30X_2^2 \quad (4)$$

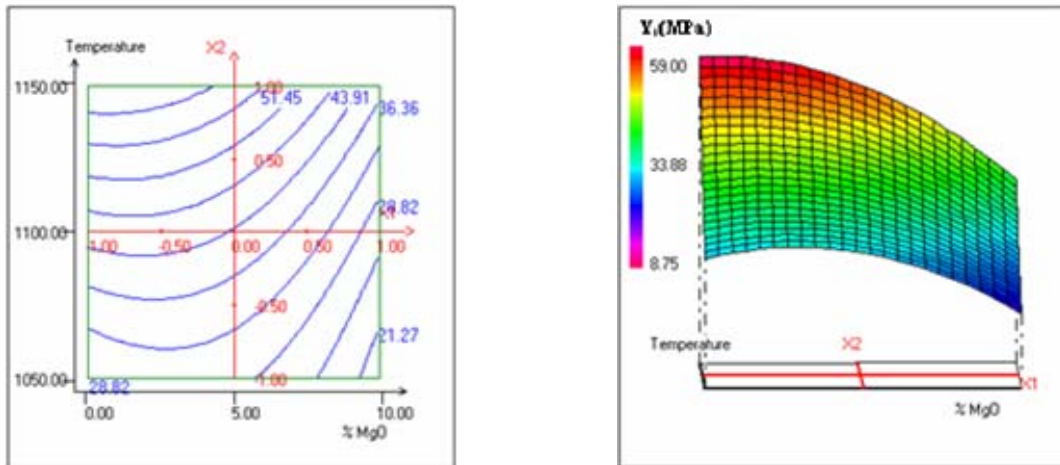


Figure 7. Iso-response curve: plot of mechanical strength versus temperature and magnesia amount

The positive sign of the coefficient (1.89) relevant to magnesia percentage shows its opposite effect on the water absorption. The water absorption increases with magnesium content increasing. These results are in agreement with the evolution of the mechanical properties described above. The negative sign of coefficient (-3.18) relevant to the temperature indicates its synergistic effect on the water absorption. The water absorption decreases with temperature increasing. The quadratic coefficients (0.55 and 0.30) indicate the presence of a stationary point. The iso-response curves (Figure 8) show the evolution of the water absorption as a function of the magnesia content and sintering temperature. We also confirm the presence of a stationary point around 2 to 3 wt%.

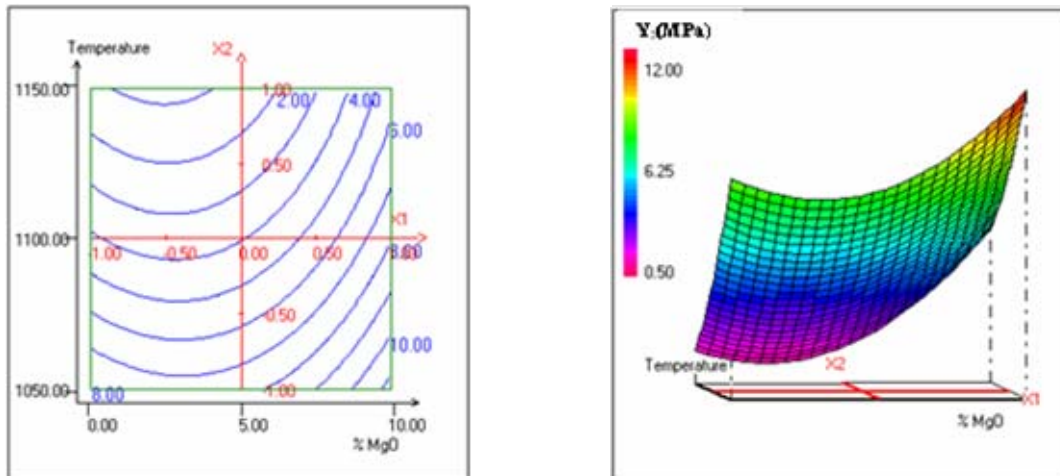


Figure 8. Iso-response curve: plot of water absorption versus temperature and magnesia amount

Microstructure

Figure 9 presents the evolution of SEM images of powders of sintered specimens with magnesia amount and sintering temperature. For all the temperatures, the number of grains increases with magnesia amount. The specimen without magnesia presents the formation of fiber characteristics of mullite. The fibers increase with temperature and the grain number decrease. At 1150 °C, we have the formation of platelets due to Mg phase's formation. The temperature increasing allows then the transformation of amorphous phase to crystalline phases. The Mg-phase and small grain increase with increasing of magnesia percentage. The different results explain the simulation results.

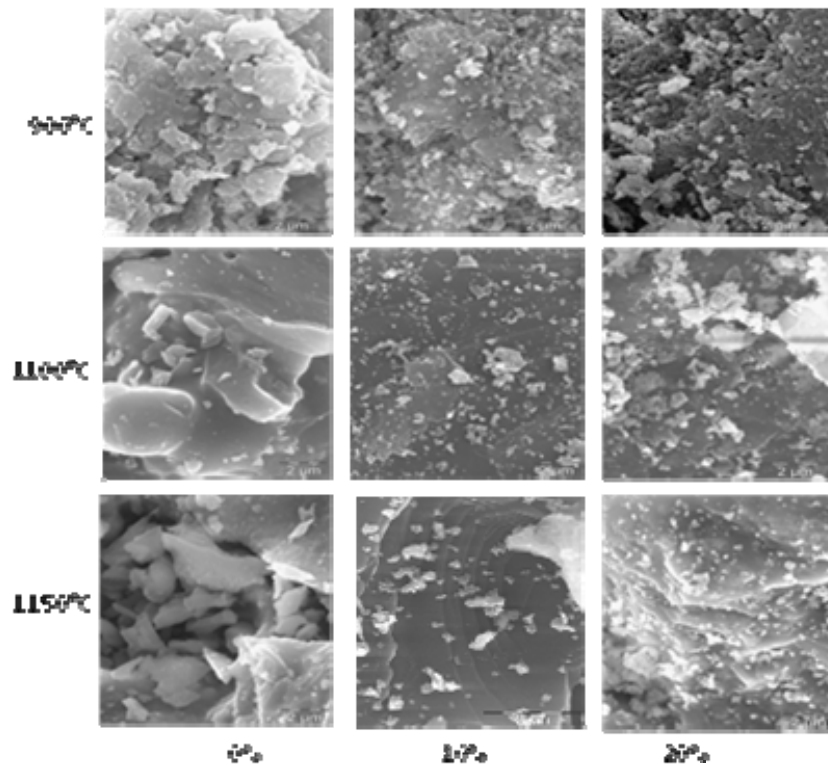


Figure 9. SEM images evolution of sintered specimen powders with magnesia amount and sintering temperature

Model validation

The analysis of the calculated and experimentally values (Table 5) shows a very good correlation between the two sets values. The analysis of variance (Table 6) shows the distribution of total calculated sums of squares. The two regression sums of squares are statistically significant. The residual sum of squares with five degrees of freedom is very feeble than the total sum of squares. The feeble value of experimental error calculated at the centre of the domain show as the previous parameters the validity of the model. The correlation coefficient ($R^2 \sim 1$) consolidates the previous results. In conclusion, the composite matrix design experience with star can be used to predict the thermo-mechanical properties of a raw clay material during it sintering.

Table 5. Experimental and calculated responses

N° Exp	% MgO	Temperature, °C	Flexural strength		Water absorption	
			Y _{exp.}	Y _{calc.}	Y _{exp.}	Y _{calc.}
1	0.00	1050.00	27.50	28.31	8.50	8.20
2	10.00	1050.00	17.50	19.15	12.00	11.38
3	0.00	1150.00	59.00	58.36	1.00	1.24
4	10.00	1150.00	37.50	37.70	5.70	5.62
5	5.00	1100.00	39.50	39.80	4.00	3.95
6	5.00	1100.00	40.70	39.80	3.80	3.95
7	-1.05	1100.00	-	-	-	-
8	11.05	1100.00	23.40	22.02	8.80	9.32
9	5.00	1039.50	30.00	28.11	7.90	8.61
10	5.00	1160.50	57.00	57.51	1.10	0.91
11	5.00	1100.00	39.50	39.80	4.10	3.95
12	5.00	1100.00	38.75	39.80	4.20	3.95

Table 6. Analysis of variance of the responses Y₁ and Y₂

Source of variation	Sum of squares	Degrees of freedom	Mean square	Ratio	Significant
Y₁					
Regression	1605.31	5	321.061	137.9560	***
Residuals	1.16363	5	2.32727		
Total	1616.94	10			
Error	1.526				
R²	0.993				
Y₂					
Regression	114.8509	5	22.9702	78.8602	***
Residuals	1.4564	5	0.2913		
Total	116.3073	10			
Error	0.540				
R²	0.987				

*** significant 99.9%

CONCLUSIONS

The contribution of magnesia on the mechanical behavior of raw clay deposit in Korona has been studied. With increasing of the sintering temperature, the specimens are consolidated by the consumption of a great part of magnesia. Mg-phases such Mg-spinel, phase, enstatite and forsterite were formed and give to the specimens the porous character. With magnesia amount between 2 and 5%, the mechanical properties were improves by forming consolidation specimen without pores. At this percentage range the material is suitable for stoneware tiles. Above 5% MgO, an important quantity of magnesia didn't react and affect the mechanical behavior. However, these products are richer in forsterite and enstatite and may well find application in the industrial field it will be important to determine their thermal and electrical conductivity.

REFERENCES

1. Sanchez, E., Garcia-Ten, J., Sanz, V., Moreno, A.: Porcelain tile: Almost 30 years of steady scientific-technological evolution, *Ceramics International*, **2010**, 36 (3), 831-845;
2. Mukhopadhyay, T.K., Das, M., Ghosh, S., Chakrabarti, S., Ghatak, S.: Microstructure and thermo mechanical properties of a talc doped stoneware composition containing illitic clay, *Ceramics International*, **2003**, 29 (5), 587-597;
3. Yang, C.-F.: The sintering characteristics of MgO-CaO-Al₂O₃-SiO₂ composite powder made by sol-gel method, *Ceramics International*, **1998**, 24 (4), 243-247;
4. Cheng, C.-M., Yang, C.-F., Lo, S.-H.: The influence of crystallization on the flexural strength of MgO-CaO-Al₂O₃-SiO₂ composite glass, *Ceramics International*, **1999**, 25 (6), 581-586;
5. Shao, H., Liang, K., Peng, F.: Crystallization kinetics of MgO-Al₂O₃-SiO₂ glass-ceramics, *Ceramics International*, **2004**, 30 (6), 927-930;
6. Vallepu, R., Nakamura, Y., Komatsu, R., Ikeda, K., Mikuni, A.: Preparation of forsterite by the geopolymer technique - Gel compositions as a function of pH and crystalline phases, *Journal of Sol-Gel Science and Technology*, **2005**, 35 (2), 107-114;
7. Petricevic, V., Gayen, S.K., Alfano, R.R., Yamagishi, K., Anzai, H., Yamaguchi, Y.: Laser action in chromium – doped forsterite, *Applied Physics Letters*, **1988**, 52 (13), 1040-1042;
8. Osborn, E.F., Muan, A.: *Revised and redrawn "Phase equilibrium diagrams of oxide systems"*, Plate 3 - System MgO-Al₂O₃-SiO₂, American Ceramic Society and the Edward Orton, Jr. Ceramic foundation, **1960**;
9. Seynou, M., Ouedraogo, R., Millogo, Y., Traoré, K., Bama, B.C.A.: Geotechnical, mineralogical, chemical and mechanical characterization of clay raw material from Korona (Burkina Faso) used in pottery, *Journal de la Société Ouest-Africaine de Chimie*, **2009**, 27, 9-19;
10. Tinsson, W.: *Plans d'expérience: constructions et analyses statistiques* (collection *Mathématiques et Applications* 67), Springer-Verlag, Berlin Heidelberg, **2010**;
11. Brindley, G.W., Hayami, R.: Kinetics and mechanism of formation of forsterite (Mg₂SiO₄) by solid state reaction of MgO and SiO₂, *Philosophical Magazine*, **1965**, 12 (17), 505-514;
12. Hosni, K., Srasra, E.: Simplified synthesis of layered double hydroxide using a natural source of magnesium, *Applied Clay Science*, **2009**, 43 (3-4), 415-419;
13. Zhang, Z., Li, N.: Effect of polymorphism of Al₂O₃ on the synthesis of magnesium aluminate spinel, *Ceramics International*, **2005**, 31 (4), 583-589;
14. Tavangarian, F., Emadi, R.: Mechanical activation assisted synthesis of pure nanocrystalline forsterite powder, *Journal of Alloys and Compounds*, **2009**, 485 (1-2), 648-652;
15. Saberi, A., Alinejad, B., Negahdari, Z., Kazemi, F., Almasi A.: A novel method to low temperature synthesis of nanocrystalline forsterite, *Materials Research Bulletin*, **2007**, 42 (4), 666-673.